

Supplementary Material

Serine racemase is associated with schizophrenia susceptibility in humans and in a mouse model

Viviane Labrie, Ryutaro Fukumura, Anjali Rastogi, Laura J. Fick, Wei Wang, Paul C. Boutros, Mawahib O. Semeralul, Frankie H. Lee, Glen B. Baker, Denise D. Belsham, Steven W. Barger, Yoichi Gondo, Albert H. Wong, and John C. Roder

Supplementary Materials and Methods

Mutation screening and mice

The TGCE system was used to screen genomic fragments spanning exons of the *Srr* gene. In exon 9, a mutation was identified using the primer pair: 5'-GGCATTGTAAACAGAACCCTG-3' and 5'-CTGCAACCAACCAAACTCC-3'. Direct sequencing with an ABI 3700 sequencer (Applied Biosystems) and data analysis with the Sequencher program (Gene Codes) confirmed the presence of a nonsense mutation at amino acid 269. Animals carrying the *Srr*^{Y269*} mutation were bred with C57BL/6J mice obtained from CLEA Japan (generation 2), and C57BL/6J mice purchased from The Jackson Laboratory (generation 3-8). Genotyping *Srr*^{Y269*} mice involved the amplification of a 363-bp PCR product using the primer pair: 5'-GCTACCAGTCTAAACTGAAAGGAGA-3' and 5'-CCAGCAGTCGGCTCAATG-3'.

Western blot analysis

Dissected whole brain, hippocampus, frontal cortex, and cerebellum tissue was homogenized in RIPA lysis buffer (Santa Cruz Biotechnology) containing protease inhibitors (Santa Cruz Biotechnology). Homogenates were centrifuged at $20,000 \times g$ for 10 min at 4°C , supernatants were collected, and protein concentrations were measured by a Bradford assay (Bio-Rad). Protein samples (50 μg) were suspended in loading buffer (Bio-Rad) containing 2-mercaptoethanol (Sigma), incubated at 95°C for 5 min, and loaded onto an SDS-PAGE gel (Criterion; Bio-Rad) along with 5 μl of MagicMark XP Western Protein Standard (Invitrogen) to be separated (100 V, ~ 2 h) using a Bio-Rad Criterion electrophoresis system (Bio-Rad). Proteins were then electrotransferred (50 V, 2 h) onto a nitrocellulose membrane (Amersham Biosciences). The membrane was blocked with 5% nonfat dry milk (Bio-Rad) in TBS-T solution (TBS, 0.1% Tween-20) for ≥ 1 h, and incubated with the primary antibody in blocking solution overnight at 4°C (Srr, PICK1, Ttr, Enpp2, Kl, Igf2, Folr1, Prlr, Otx2, Cldn2) or for 2 h at room temperature (NR1, GluR1, GluR2, GlyT-1, DAO). Following washes with TBS-T (3×10 min), the membrane was incubated for 1 h with the appropriate horseradish peroxidase-conjugated secondary antibody: anti-mouse IgG (GE Healthcare; 1:5,000 in blocking solution), anti-rabbit IgG (GE Healthcare; 1:5,000 in blocking solution), anti-goat IgG (Santa Cruz Biotechnology; 1:3,000). The membrane was washed in TBS-T (3×10 min) and then processed for chemiluminescence using a Western blotting detection kit (GE Healthcare). Equal loading was confirmed by immersing the membrane in Restore Western Blot Stripping Buffer (Thermo Fisher Scientific) prior to incubation with a rabbit anti- β -tubulin III polyclonal antibody (Sigma; 1:20,000 in blocking solution for 1 h). Exposure of the membrane to photographic film permitted for visualization of protein bands that were then quantified by densitometric analysis

using the Image J 1.41 software (<http://rsbweb.nih.gov/ij/>). Each densitometric value was normalized to its respective β -tubulin III loading control.

RNA isolation

Total RNA was isolated from whole brain, hippocampus, frontal cortex, and cerebellum using Trizol reagent (Invitrogen) according to the manufacturer's instructions. For the microarray experiment, additional purification of total RNA was completed with the Absolutely RNeasy RT-PCR Miniprep kit (Stratagene). RNA yield was quantified by UV spectrophotometry (NanoDrop ND-1000; Thermo Fisher Scientific) and RNA integrity was verified using the Agilent Bioanalyzer 2100 system (Agilent Technologies).

Real time RT-PCR

Total RNA from whole brain and hippocampus was used for real-time PCR reactions. RNA samples (2 μ g) were initially DNase treated (Turbo DNase, Ambion) for 30 min at 37°C, and then incubated with 5 mM EDTA at 75°C for 10 min to inactivate DNase I. The DNase-treated RNA was used as a template to generate a cDNA archive using the High Capacity cDNA Archive kit (Applied Biosystems). Following cDNA generation, gene expression was assayed in triplicate on a 7900HT Fast Real Time PCR System (Applied Biosystems). Genes were amplified with Platinum *Taq* (Invitrogen) and quantitative RT-PCR reagents (Invitrogen), and expression was normalized to housekeeping genes (18s rRNA, γ -actin, histone 3a). Three housekeeping genes were utilized to rule out potential genotype specific effects in housekeeping gene expression. Primer sequences for quantitative analysis of the following genes were: *Srr* (5'-AGGCCCTGAAACCTAGTGTGAA-3', 5'-TTCATTCTCCCCCACACCA-3'), *PICK1* (5'-

CGAGGAATACAGCTGCATTGC-3', 5'-CGCAGAATGAGGCGGTACTC-3'), transthyretin (5'-TTCCATGAATTCGCGGATGT-3', 5'-AGCCGTGGTGCTGTAGGAGTAT-3'), ectonucleotide pyrophosphatase/phosphodiesterase 2 (5'-TCTGTATACGCTGGCCACTGGT-3', 5'-CGCCCTCGAAGATGGAAAGTA-3'), klotho (5'-AGCCAATGGAATCGATGATGAC-3', 5'-CCAACACGTAGGCTTTCAGAGC-3'), insulin-like growth factor 2 (5'-TTGTGCTGCATCGCTGCTTAC-3', 5'-AAGGCCTGCTGAAGTAGAAGCC-3'), folate receptor 1 (5'-GGGCATAACGAGTGTCCCTGT-3', 5'-GCTCCCTCGACTGTAGTTGC-3'), prolactin receptor (5'-AACTGTGTGCATCATTGTGGCC-3', 5'-GGAAAGATGCAGGTCATCATGC-3'), orthodenticle homolog 2 (5'-GTTCTGGAAGCTCTGTTTGCCA-3', 5'-AAACCATACCTGCACCCTGGA-3'), claudin 2 (5'-TGACGTCCAGTGCAATGTCCT-3', 5'-AGCCACTCTGTCCTTAGCTCGA-3'), serum/glucocorticoid regulated kinase 1 (5'-ACATCTACCTTCTGTGGCACGC-3', 5'-TCTCATAACAGGACAGCCCCAAG-3'), 18s rRNA (5'-GTAACCCGTTGAACCCCAT-3', 5'-CCATCCAATCGGTAGTAGCG-3'), γ -actin (5'-CTTCCCCACGCCATCTTG-3', 5'-CCCGTTCAGTCAGGATCTTCAT-3'), and histone 3a (5'-CGCTTCCAGAGTGCAGCTATT-3', 5'-ATCTTCAAAAAGGCCAACCAGAT-3').

Srr activity

Brain samples were homogenized in 5 volumes of ice-cold buffer A [50 mM Tris-HCl, pH 8.0, 50 mM KCl, 1 mM EDTA, 2 mM dithiothreitol (DTT), 15 μ M pyridoxal L-phosphate (PLP), 0.2 mM phenylmethylsulfonyl fluoride, 1 μ g/ml leupeptin, 1 μ g/ml aprotinin] and centrifuged at $20,000 \times g$ for 30 min at 4°C. Supernatants were measured for protein concentrations and equalized prior to a two-step ammonium sulfate purification. Saturated $(\text{NH}_4)_2\text{SO}_4$ was added to

a final concentration of 20%; samples were mixed by gentle rotation for 2 h at 4°C, then centrifuged at $14,000 \times g$ for 10 min at 4°C to remove the pellets. Afterwards, the concentration of $(\text{NH}_4)_2\text{SO}_4$ in the supernatants was raised to 45%, and samples were rotated for 1 h at 4°C, then left unstirred at 4°C overnight. Pellets were collected by centrifugation at $14,000 \times g$ for 10 min at 4°C, then resuspended in 320 μl of buffer B (50 mM Tris-HCl, pH 8.0, 50 mM KCl, 0.1 mM DTT, 15 μM PLP). Samples were dialyzed against 1000 ml of buffer B for 2 h at 4°C, and protein concentrations were measured in each sample.

Srr reactions were performed with enriched L-serine as a substrate. To minimize the levels of the D-serine that contaminates virtually all L-serine preparations, commercially obtained L-serine (Sigma) was reacted with porcine DAO (Calzyme Laboratories) as follows: Up to 20 μmol of L-serine was combined with 1.5 U/ml porcine DAO, 3 U/ μl catalase (Sigma) and 84 $\mu\text{g}/\text{ml}$ flavin adenine dinucleotide (Calbiochem) in buffer C (0.15 M Tris-HCl, pH 8.3); the mixture was incubated at 37°C overnight, then at 95°C for 10 min. The supernatant was collected after centrifugation at $17,000 \times g$ for 10 min. Removal of D-serine was confirmed by a D-serine chemiluminescent assay (below). This enriched L-serine was combined with 1 mM ATP, 1 mM MgCl_2 , and 1 mM CaCl_2 in buffer B. Srr reactions were initiated by addition of brain protein samples (100 μg), incubated at 37°C for 2 h, and then stopped by incubation for 5 min at 100°C.

A chemiluminescent assay was then used to measure D-serine levels in the Srr reactions. Buffer D (100 mM Tris-HCl, pH 8.8, 50 mM NaCl) containing 0.1 U horseradish peroxidase (Sigma), 0.8 nmol luminol (Sigma), and 0.048 nmol flavin adenine dinucleotide (Calbiochem) was diluted into each Srr reaction at a 1:5 ratio. A Veritas Microplate Luminometer (Turner Biosystems) was used to detect the production of H_2O_2 before and after the addition of 0.002 U

R. gracilis DAO (courtesy of L. Pollegioni, U. Insubria, Varese, Italy). Triplicates of each sample were measured, and the content of D-serine was quantified using a calibration curve of D-serine standards.

HPLC

Brain samples were homogenized in 5 volumes of ice-cold double distilled water. An aliquot was mixed with 100% methanol to give a final dilution of 60× and then centrifuged at 12000 × g for 4 min at 4 °C. A 5 µl aliquot of the supernatant was mixed with 5 µl of the derivatizing reagent (2 mg N-isobutyryl-L-cysteine and 1 mg o-phthaldialdehyde dissolved in 0.1 ml methanol, followed by addition of 0.9 ml 0.1 M sodium borate buffer), and then was placed into a sample management system (Waters Alliance 2690XE, Waters). HPLC separation was achieved on a Symmetry C18 column (4.6 mm×150 mm; 3.5 µm particle diameter) coupled with a guard column of the same stationary phase (Waters). The column heater was set at 30 °C and the sample cooler was held at 4 °C. To separate the derivatized amino acids of interest, a gradient was established from equal parts of solvent A (850 ml of 0.04 M sodium phosphate buffer and 150 ml methanol, pH 6.2) and B (670 ml of 0.04 M sodium phosphate buffer, 555 ml methanol and 30 ml tetrahydrofuran , pH 6.2) to only solvent B by ~45 min, with a flow rate of 0.5 ml/min. The run time was 60 min for column washout and equilibrium, and 30 min to elute all compounds. A Waters 2475 fluorescence detector (Waters) was used to quantify the eluted compounds (excitation 344 nm; emission 433 nm).

Behavioral studies

Prior to experiments, mice were left undisturbed in the room for at least 30 min to allow for acclimatization. Where possible, the experimental equipment was cleaned with 70% ethanol between each subject.

Physical assessment. A physical examination that included evaluation of sensory functions and reflexes was completed to detect any gross abnormalities. Weights were measured in mice that were 8, 12, and 18 weeks of age. All other measures in this assessment were completed on mice that were 8 weeks of age. The presence and condition of fur and whiskers was assessed visually. The eye-blink reflex was examined by approaching an eye with the end of a cotton swab, causing the immediate blink of that eye. The ear-twitch reflex was examined by approaching an ear from behind with a cotton swab that would then touch the pinna, resulting in immediate movement of that ear. The whisker-twitch reflex was examined by gently touching the ends of one set of vibrissae, resulting in cessation of vibrissae movement and a head turn towards the touched side. The righting reflex was examined by turning the mouse on its back, causing the immediate regain of an upright posture. Vision was assessed using the visual placing test, where vision was considered to be normal in mice (>80% group criteria) that would reach for a passing table surface, after being lowered 15 cm above and 4 cm out from the table surface.

Accelerating rotarod. The rotarod apparatus (Economex Rotarod; Columbus Instruments) had a ribbed rotating axle (3 cm diameter) that was situated 30 cm above a plastic surface. A maximum of four mice could be tested simultaneously with each mouse being separated by an opaque wall (30 cm width×60 cm height). Mice were placed on the rod facing away from the experimenter and initially allowed to acclimatize to the stationary rod for 60 s. The axle was

then set at a constant speed of 5 rpm for 90 s. Afterwards, the axle speed (starting at 5 rpm) was increased by 0.1 rpm/s and the latency to fall off the axle was recorded for each mouse, with a maximum of 360 s in the acceleration mode. On each day, 3 trials were completed with a 1-h intertrial interval. Motor coordination and balance was evaluated by comparing the mean latencies to fall from the rod (average of the 3 daily trials). Motor learning was determined by observing an improved latency on the last day compared to the first day (motor learning ratio = latency day 3 / [latency day 1 + 3]). Impaired performance in the stationary and constant speed sessions was considered to be an early indicator of motor abnormality.

Locomotor activity. The testing period began by placing a mouse individually at the center of the automated activity cage. The mouse was allowed to freely explore the apparatus for the duration of the test.

Forced swim test. Mice were placed into a cylinder (25 cm height, 18 cm diameter) containing water (26°C) at a depth of 18 cm for a duration of 6 min. The time spent immobile, as defined by floating in an upright position with only minimal movements necessary for the head to remain above water, was recorded during the last 4 min of the test period. The water was changed between each subject. Testing sessions were video recorded, and data was collected and analyzed using an event-recording program (Observer 5.0; Noldus).

Elevated plus-maze. The apparatus used in elevated plus-maze test consisted of two open arms (25×5 cm; 70 lx) and two closed arms (25×5×30 cm; 1.3 lx) extending from a central platform (5×5 cm) and elevated 50 cm from the ground. The floor of the arms was made of white

Plexiglas and the walls of the closed arms were made of black Plexiglas. Similar arms were opposite to each other and at a 90° angle from dissimilar arms. The test mouse was placed in the central area facing an open arm and allowed to explore the apparatus for 5 min. The number of entries and the time spent in the open arms, closed arms, and central platform was recorded and analyzed using the Observer 5.0 program (Noldus) and videotaped. An entry was defined as placing all four paws within one arm of the maze. Anxiolytic effects were assessed by an increase in % open arms time ($[\text{open arm time} / \text{total time on apparatus}] * 100$) and in % open arm entries ($[\text{open arm entries} / \text{total arm entries}] * 100$), whereas anxiogenic effects were indicated by a decrease in these measures. Total number of entries (open + closed arm entries) was used as a measure of overall motor activity.

Social affiliations. The social affiliations task was conducted in a clear Plexiglas box (61.5 cm length×46 cm width×23 cm height) divided into three interconnected chambers (outer chambers=19 cm length, central chamber=23.5 cm length). The outer chambers were identical to each other and divided from the central chamber by clear Plexiglas partitions (17.5 cm width×23 cm height) that each had a centrally placed opening (11 cm width×23 cm height) and a retractable chamber divider. Transparent Plexiglas cages with a cylindrical shape (13 cm height, 8 cm diameter) were used to contain the stranger mice and were perforated with evenly distributed holes (1 cm diameter). Throughout the experimental sessions, the cages were located at the center of each outer chamber and permitted auditory, visual, and olfactory investigation.

The stranger mice used were age-matched, male C57BL/6J mice (The Jackson Laboratory) that had never been in contact with the test subjects. At the beginning of each experimental session, the test mouse was placed in the central chamber and was allowed to freely

explore for 10 min. Data were not recorded during this habituation period. Afterwards, the experimenter placed a stranger mouse (stranger 1) in one of the cages and handled the other empty cage similarly. The cage and outer chamber containing the stranger mouse was alternated across subjects. After the placement of the stranger mouse, the test subject explored the social apparatus for 10 min (sociability phase). The test mouse was considered to be in a chamber if its head and two front paws had entered the chamber. The amount of time spent investigating each chamber, the number of entries into each chamber, freezing, and grooming were scored using the Observer 5.0 software (Noldus) and video recorded.

Preference for social novelty was also examined. Immediately after the sociability assessment detailed above, a second unfamiliar mouse (stranger 2) was placed beneath the previously empty cage (social novelty phase). The test mouse could now explore the central chamber, the chamber containing the initial stranger (stranger 1; now familiar), or the chamber containing a novel stranger (stranger 2) for a period of 10 min. All other parameters and measures were as described above in the sociability phase.

Olfactory test. Mice were given a 24-h food deprivation period before testing. In the experiment, clean polycarbonate cages (30×17×12 cm) with fresh corncob bedding were used for each subject. One piece (approximately 1×1×1 cm) of Lab Diet rodent chow (PMI Nutrition International) was buried in a random location beneath an evenly distributed layer of corncob bedding (2.5 cm in depth). The latency to find the buried food was recorded, with a maximum period of 10 min.

Prepulse inhibition. Acoustic startle response and PPI were tested using 4 sound-attenuating chambers (ENV-022s; MED Associates). Each chamber contained an acoustic stimulator (ANL-925) and an amplified load cell platform (PHM-255A and PHM-250B). Chambers were also equipped with a fan and a red light. Mice were placed into ventilated holders (ENV-263) that were attached to the platform of each chamber. Data acquisition and analysis employed the MED Associates software (Startle Reflex package).

Testing sessions began by individually placing mice into the startle chambers. Mice were given a 15-min acclimatization period to background noise (65 dB). Afterwards, subjects were presented with a series of five startle-pulse-alone (P) trials, each comprised of a single white noise burst (120 dB, 40 ms). This was followed by a series of trials consisting of no stimulus (background noise, 65 dB), a startle-pulse-alone, or one of three prepulse intensities (69, 73, and 81 dB, 20 ms) presented 100 ms before a startle-pulse (120 dB, 40 ms). This series of trials was given in 10 blocks each containing all five trial types (no stimulus, P, 69 dB + P, 73 dB + P, 81 dB + P) in pseudorandom order. Finally, an additional series of five startle-pulse-alone trials were presented. Intertrial intervals were between 12 to 30 s. The peak startle activity for each trial was recorded. PPI was expressed as the reduction in startle amplitude in prepulse + pulse trials compared to startle-pulse-alone trials. The % PPI for each prepulse intensity was calculated according to the following formula: $\%PPI = 100 - (\text{startle response on prepulse trials} / \text{startle response on startle-pulse-alone trials}) \times 100$. To measure startle reactivity, mice were acclimatized to the testing chamber for 15 min prior to the presentation of startle stimuli of varying intensities (70-120 dB), with a 25-ms duration and an inter-stimulus interval of 25-30 s. Startle stimuli were presented in three blocks each composed of two demonstrations of the 11

stimulus intensities given in pseudorandom order. The average startle amplitude for each stimulus intensity was calculated from the three blocks.

Spatial and nonspatial recognition. The spatial and nonspatial discrimination task was performed in the apparatus used to measure locomotor activity. The five objects used in this task differed in shape, color, and material (approximately 7×5×5cm). Animal behavior was recorded and analyzed using The Observer 5.0 (Noldus).

On test day, each mouse was individually placed in the center of the empty arena for a 5-min session (S1), and locomotor activity (beam breaks) was recorded. The mouse was then placed in a holding cage for 2 min. Four objects were placed in specific positions near each corner of the arena (5 cm from corner walls). The mouse was returned to the center of the arena and allowed to explore the objects for three continuous 5-min sessions (habituation phase, S2–S4). Habituation to object exploration was measured by recording the time spent exploring the objects across sessions S2–S4. A mouse was considered to be exploring an object if its snout was in contact with the object. Duration of locomotor activity was also measured during these sessions (S2–S4) and in subsequent sessions. At the end of S4, the mouse was again placed in the holding cage for 2 min and the position of two objects (NW and SE or NE and SW) was switched to assess response to a spatial change. During the switch, all four objects were touched by the experimenter and objects that were moved were counterbalanced within groups. The mouse was returned to the arena, and the time spent exploring the displaced and non-displaced objects was recorded for 5 min (spatial change phase, S5). Reaction to a spatial change was assessed by comparing the mean time spent exploring the displaced and non-displaced object categories.

Reactivity to a nonspatial change was also examined. Directly after S5, the test subject was returned to the holding cage for 2 min, during which one of the familiar non-displaced objects in the arena was replaced by a novel object in the same location. The mouse was returned to the center of the arena for a 5-min period (nonspatial change phase, S6). Measurements were taken as described for S5, and the response to nonspatial change was evaluated by considering the mean time spent exploring the novel object and the three familiar objects.

Morris water maze. The Morris water maze (MWM) consisted of a white Plexiglas, cylindrical pool (1.2 m diameter) that was filled with opaque water ($26^{\circ}\text{C} \pm 1^{\circ}\text{C}$). The pool was arbitrarily divided into four equal quadrants: northeast, northwest, southeast, and southwest. The circular escape platform (10 cm diameter) was made of clear Plexiglas. Distal visual cues were fixed on each wall ~ 1 m from the pool edge. Activity in the water maze was recorded using a CCD camera on the ceiling above the center of the pool attached to an automated tracking system (HVS Image) that extracted and stored the X-Y coordinates of the subject every 0.01 s. The HVS Water 2020 software (HVS Image) was used to establish experimental parameters and analyze performance. Behavioral measures in the MWM included latency to target (s), path length (m), thigmotaxis (% time within 8 cm of the pool wall), swim speed (cm/s), floating (% time), % time within the target area, and number of platform crosses.

Subjects were handled for 2 min/day on each of the 5 consecutive days prior to testing. Each MWM procedure began with a 1-day stationary visible platform task. Mice were given 4 trials with a ~ 1 -h intertrial interval. In each trial, mice were released facing the pool wall from one of four pseudo-randomized locations (N, S, W, E) at the pool periphery. The platform was

at the center of the target quadrant (NW) and 25 cm from the pool wall. In the visible trials, the platform was raised 0.5 cm above the water surface and demarcated with a 10 cm vertical pole. The maximum duration for a platform search was 90 s. Animals that found the platform remained on it for an additional 15 s, whereas unsuccessful animals were assigned a 90-s latency and gently placed onto the platform for 15 s. The acquisition phase began 1 day later, and lasted for 7 consecutive days (4 trials/day, 1 h intertrial interval). Each day was performed similarly to the visible platform task, except the platform was now submerged ~1 cm below the surface of the water (hidden) in the NW quadrant. Retention of spatial memory was assessed in a 60-s probe trial that occurred 24 h after acquisition day 5 and day 7. In the probe trials, the platform was removed and mice were released from the point furthest (SE) from the former platform location. Performance in the probe trial was quantified by examining the % time spent and number of crosses over an area that was three times the platform diameter, centered over its former location.

Statistical analysis of biochemical and behavioral data

Statistical analyses were performed using Statistica (Statsoft). Biochemical (Figure 1 and supplemental Figure 2) and behavioral data were analyzed using one-way, two-way, or repeated-measures (RM) ANOVA with the appropriate between-subjects and within-subjects factors. Significant main effects or interactions were followed by Fisher's least significant difference (LSD) post hoc comparisons.

Microarrays

Biotinylated and amplified cRNA was generated using the Illumina TotalPrep RNA Amplification Kit (Applied Biosystems). Labeled cRNA samples (750 ng) were then hybridized to arrays in accordance with manufacturer protocols for hybridization, staining, and data acquisition. Arrays were imaged using the Illumina BeadArray Reader (Infinium I FastScan scanner protocol), a two-channel 0.8 μm resolution confocal laser scanner. The BeadScan software (Illumina) was used for the identification of bead positions and the extraction of raw data.

Illumina data were pre-processed separately and identically for each tissue. All pre-processing was performed in the R statistical environment (v2.7.2) using the BioConductor open-source library (1). Raw array data (TIFF files) were first processed using the beadarray package (v1.8.0) (2). The raw data were subsequently background-corrected using the non-linear Edwards model (3). Following careful quality assessment at the bead and gene level, no arrays were excluded. The background-corrected data were summarized in normal space using the standard Illumina method. The summarized data were transformed using the vst method as implemented in the lumi package (v1.6.2) (4), and then normalized using quantile splines (5).

To identify mRNAs exhibiting differential abundance between the wild-type and mutant mice we employed the RankProducts algorithm (6), as implemented in the RankProd package (v2.12.0). The percentage of false-positives (PFP) was determined using 1000 permutations (default is 100) and used as a multiple-testing adjusted measure of the false-discovery rate. Results were then aggregated across the three tissues and associated with updated bead annotation obtained from: <http://www.compbio.group.cam.ac.uk/Resources/illumina/index.html>. A significance threshold of $\text{pfp} < 0.05$ was set. Genes differentially expressed in at least one of three tissues were subjected to divisive hierarchical clustering using the DIANA algorithm

(cluster package, v1.11.11) and Pearson's correlation as a distance metric. Clustering results were visualized with heatmaps using the lattice (v0.17-15) and latticeExtra (v0.5-2) packages for the R statistical environment.

To associate differentially expressed genes with functional groupings we employed GO enrichment analysis using the GOMiner package (7). We employed build 209 of the application and database build 2008-04, using 1000 permutations to estimate the false-discovery rate. All murine databases, evidence codes, and ontologies were tested. Separately, we also assessed these genes in the Reactome database; no statistically significant enrichments were detected (data not shown).

Human SNP analysis

Patients were recruited from the greater Toronto, Ontario area. Small nuclear families consisted of 35 triads, 9 triads plus a sibling where two of the siblings were affected with schizophrenia, 54 diads, 8 families with an affected proband plus single parent plus sibling where all the siblings were unaffected, and 11 families with a proband plus sibling where two siblings were affected. In the case-control sample, patients and control subjects were matched for age, gender and self-reported ethnicity (8) to minimize the chance of population stratification from heterogeneous case and control groups. The Structured Clinical Interview for DSM-IV (SCID-I) (9) was conducted by an experienced clinical team, and was used as a primary diagnostic tool for this study. Additionally, a clinical summary providing detailed information concerning the sequence, context, and severity of symptoms was prepared for each patient (10). The diagnosis was established following review of the SCID-I and clinical summary by research psychiatrists. Patients that satisfied the DSM-IV diagnostic criteria for schizophrenia were included in the

study (11), while patients with history of major substance abuse, major neurological disorders or head injury with significant loss of consciousness were excluded. Control subjects were screened using the Family Interview for Genetic Studies (10) and excluded if there was any personal or family history of mental illness or substance/alcohol abuse.

The tagSNP selection from the International HapMap Project genotyping data (www.hapmap.org) in a CEU population (Utah residents with ancestry from northern and western Europe) was used to choose SNP markers in the *Srr* gene ($r^2 < 0.8$ and minor allele frequency > 0.1). TaqMan assays (Applied Biosystems) consisting of primers, VIC dye and FAM-labeled probes were used in a PCR amplification protocol (95°C for 10 min followed by 50 cycles of 92°C for 15 sec and 60°C for 1 min).

The chi-square test in Haploview version 3.2 (12) was used to test for concordance with the Hardy-Weinberg equilibrium (HWE), calculate linkage disequilibrium (LD), create the LD blocks, and perform the case-control analysis. Haplotype analyses for the case-control sample were conducted using the COCAPHASE (UNPHASED 3.0.10) (13). Genetic association in the family sample was analyzed using the family-based association test (FBAT) bi-allelic additive model (14) and haplotypes were analyzed with the HBAT command from FBAT. To account for the multiple haplotypes tested, global p -values were obtained from permutation analysis ($< 10,000$ permutations). A Bonferroni correction for multiple comparisons was applied to significant genetic associations (15).

Supplementary References

1. Gentleman, R.C., Carey, V.J., Bates, D.M., Bolstad, B., Dettling, M., Dudoit, S., Ellis, B., Gautier, L., Ge, Y. and Gentry, J., et al. (2004) Bioconductor: open software development for computational biology and bioinformatics. *Genome Biol.*, **5**, R80.
2. Dunning, M.J., Smith, M.L., Ritchie, M.E. and Tavare, S. (2007) Beadarray: R classes and methods for Illumina bead-based data. *Bioinformatics*, **23**, 2183-2184.
3. Edwards, D. (2003) Non-linear normalization and background correction in one-channel cDNA microarray studies. *Bioinformatics*, **19**, 825-833.
4. Lin, S.M., Du, P., Huber, W. and Kibbe, W.A. (2008) Model-based variance-stabilizing transformation for Illumina microarray data. *Nucleic Acids Res.*, **36**, e11.
5. Workman, C., Jensen, L.J., Jarmer, H., Berka, R., Gautier, L., Nielser, H.B., Saxild, H.H., Nielsen, C., Brunak, S. and Knudsen, S. (2002) A new non-linear normalization method for reducing variability in DNA microarray experiments. *Genome Biol.*, **3**, research0048.
6. Breitling, R., Armengaud, P., Amtmann, A. and Herzyk, P. (2004) Rank products: a simple, yet powerful, new method to detect differentially regulated genes in replicated microarray experiments. *FEBS Lett.*, **573**, 83-92.
7. Zeeberg, B.R., Feng, W., Wang, G., Wang, M.D., Fojo, A.T., Sunshine, M., Narasimhan, S., Kane, D.W., Reinhold, W.C. and Lababidi, S. (2003) GoMiner: a resource for biological interpretation of genomic and proteomic data. *Genome Biol.*, **4**, R28.
8. Rosenberg, N.A., Pritchard, J.K., Weber, J.L., Cann, H.M., Kidd, K.K., Zhivotovskiy, L.A. and Feldman, M.W. (2002) Genetic structure of human populations. *Science*, **298**, 2381-2385.
9. First, M.B., Gibbon, M., Spitzer, R.L. and Williams, J.B.W. (1996) *Structured clinical interview for DSM-IV axis I disorders, research version (SCIDI/P), second edition*. American Psychiatric Press, Washington, D.C.
10. Maxwell, M.E. (1992) Family interview for genetic studies: The NIMH molecular genetic initiative., <http://www.grb.nimh.nih.gov/interviews.html>.
11. APA (1994) *Diagnostic and statistical manual of mental disorders, fourth edition*. American Psychiatric Association, Washington, D.C.
12. Barrett, J.C., Fry, B., Maller, J. and Daly, M.J. (2005) Haploview: analysis and visualization of LD and haplotype maps. *Bioinformatics*, **21**, 263-265.
13. Dudbridge, F. (2003) Pedigree disequilibrium tests for multilocus haplotypes. *Genet. Epidemiol.*, **25**, 115-121.
14. Horvath, S., Xu, X., Lake, S.L., Silverman, E.K., Weiss, S.T. and Laird, N.M. (2004) Family-based tests for associating haplotypes with general phenotype data: application to asthma genetics. *Genet. Epidemiol.*, **26**, 61-69.
15. Benjamini, Y., Drai, D., Elmer, G., Kafkafi, N. and Golani, I. (2001) Controlling the false discovery rate in behavior genetics research. *Behav. Brain Res.*, **125**, 279-284.

Supplementary Figure Legends

Figure S1. A nonsense mutation in exon 9 of murine *Srr*. **(A)** DNA sequence chromatograms depicting the mutation in *Srr*. Near the start of exon 9, a transversion (A → T) occurred, which converted amino acid 269 from a tyrosine (TAA) to a stop codon (TAT). DNA sequences for both wild-type (+/+) and homozygous mutant mice (Y269*/Y269*) are shown for comparison. **(B)** Mouse and human *Srr* protein sequences were aligned using the ClustalX2 program for homology comparison. Identical residues are marked in gray. The position of the *Srr*^{Y269*} mutation in mice is indicated with red text and an arrow. A line indicates a gap in the alignment, and the blue and black text distinguishes the exons.

Figure S2. Biochemical alterations in *Srr*^{Y269*} mutant mice. **(A1)** Western blot using a polyclonal *Srr* antibody to probe protein extracts from whole brain of wild-type (+/+), heterozygous (+/Y269*), and mutant (Y269*/Y269*) mice. Substantial loss of *Srr* protein was found in mutant mice. β -Tubulin III was used as a loading control. The molecular weights in kiloDaltons (kDA) of *Srr* and a protein standard (S) are marked. **(A2)** Densitometric quantification of Western blot for *Srr*. The mean densitometry (\pm SEM) indicates the levels of *Srr* protein in wild-type, heterozygote, and mutant animals (genotype, $F_{2,6} = 563.4$, $P < 0.001$). *** $P < 0.001$ compared to wild-type mice; #### $P < 0.001$ compared to heterozygous mice. **(B)** Real-time RT-PCR analysis of *Pick1* mRNA. Mean levels of *Pick1* mRNA (\pm SEM) were measured in whole brain of wild-type (n = 6), heterozygous (n = 7), and mutant mice (n = 6), and were not significantly elevated in mutant animals.

Figure S3. Western blots examining proteins that modulate D-serine and NMDAR-mediated neurotransmission. Protein extracts from whole brain (**A1**), hippocampus (**B1**), frontal cortex (**C1**), and cerebellum (**D1**) of wild-type, heterozygous, and mutant mice were assessed for levels of NR1, GluR1, GluR2, GlyT-1, and DAO. No changes were observed in the whole brain, hippocampus, or frontal cortex. Lower levels of GlyT-1 were found in the cerebellum of heterozygous and mutant mice. A trend indicating a decreased amount of DAO in the cerebellum of mutant mice was also observed ($P = 0.06$). β -Tubulin III was used as a loading control. Densitometric quantification of Western blots for NR1, GluR1, GluR2, GlyT-1, and DAO in whole brain (**A2**), hippocampus (**B2**), frontal cortex (**C2**), and cerebellum (**D2**). The mean densitometry (\pm SEM) denotes the quantity of measured proteins in wild-type, heterozygous, and mutant mice. $*P < 0.05$ compared to wild-type mice, within the same gene.

Figure S4. Performance of mutant mice in behavioral measures of motor function, depression, and anxiety. **(A)** Mean weight of wild-type (+/+; $n = 9$) and mutant mice (Y269*/Y269*; $n = 8-13$) was similar at 8, 12, and 18 weeks of age. **(B)** Mean latency to fall from an accelerating rotarod (3-day procedure with 3 trials/day). No significant differences were observed between wild-type ($n = 14$) and mutant mice ($n = 9$), though mutant mice did demonstrate a trend towards a reduced latency to fall from the rotating axle (genotype, $F_{1,21} = 3.5$, $P = 0.08$). **(C)** The average motor learning ratio demonstrates that wild-type ($n = 14$) and mutant mice ($n = 9$) did not differ in their ability to improve their performance in the accelerating rotarod task across the 3 days. **(D)** The mean number of beam breaks during a 30-min assessment of locomotion (5-min bins) was similar in wild-type ($n = 8$) and mutant mice ($n = 12$). **(E)** The mean time of immobility of

wild-type (n = 9) and mutant mice (n = 10) did not differ in the forced swim test, an assessment of depressive-like behavior. In the elevated plus-maze, the mean time spent in the open arms (**F**) and the mean number of open arm entries (**G**) are measures of anxiety-like responses and were similar in wild-type (n = 16) and mutant mice (n = 17). (**H**) The mean number of entries in the open and closed arms, an indicator of exploratory activity, was comparable in wild-type and mutant mice during the elevated plus-maze task. Data are shown as mean \pm SEM.

Figure S5. Mutant mice in behavioral tests relevant to schizophrenia. Exploratory activity in the sociability (**A**) and social novelty session (**B**) of the social affiliations task. Mean number of chamber entries did not differ between wild-type (+/+; n = 13) and mutant mice (Y269*/Y269*; n = 12). (**C**) In a test of olfactory acuity, the mean latency to uncover a buried food pellet was similar wild-type (n = 14) and mutant animals (n = 7), indicating similar olfactory function. (**D**) Acoustic startle response of wild-type (n = 13) and mutant mice (n = 12). Mean startle amplitude in response to a stimulus (120 dB) given in absence of a prepulse did not differ between wild-type and mutant animals. (**E**) Acoustic startle response to varying stimulus intensities (70 – 120 dB) administered without a prepulse. Reactivity of wild-type (n = 14) and mutant animals (n = 9) similarly increased with greater stimulus intensities, indicative of normal hearing (stimulus intensities, $F_{10,210} = 24.3$, $P < 0.001$). (**F**) In the open field session (S1) of the object recognition task, the mean number of beam breaks in the empty arena was not different between wild-type (n = 8) and mutant mice (n = 11). (**G**) Duration of locomotor activity during the sessions of habituation (S2-S4), spatial change (S5), and non-spatial change (S6) in the object recognition task was comparable between wild-type and mutant mice. (**H**) In the habituation sessions (S2-S4) of the object recognition task, the mean duration of object exploration for wild-

type and mutant mice showed a similar progressive acclimatization to all four objects (session, $F_{2,34} = 97.0, P < 0.001$). Analysis of the time spent investigating each individual object revealed that exploration did not favor any object (genotype \times session \times object, $F_{6,102} = 0.2, P = 1.0$). **(I)** During the last habituation session (S4) of the object recognition task, the mean time spent exploring the objects that will be displaced or non-displaced in the subsequent spatial change session demonstrated that wild-type and mutant mice have no bias for either object category. **(J)** Mean path length to reach a target platform in a visible platform session (day 1), and in a hidden-platform acquisition training phase (days 2-8) of the MWM. Performance in these training trials did not differ between wild-type ($n = 14$) and mutant mice ($n = 13$). No differences were observed in swim speed (genotype in acquisition trials, $F_{1,25} = 0.6, P = 0.4$), floating ($F_{1,25} = 0.1, P = 0.7$), and thigmotaxis ($F_{1,25} = 0.3, P = 0.6$), indicating that the *Srr^{Y269*}* mutation did not alter sensorimotor abilities or search motivation. Probe sessions were administered 24 h after days 6 and 8, as indicated by an arrow. The probe trials **(K and L)** were conducted to assess spatial memory retention. **(K)** In probe trial 1, wild-type mice spent more time in the correct target location relative to mutant mice and relative to the averaged analogous non-target locations (genotype, $F_{1,25} = 5.9, P < 0.05$). **(L)** In probe trial 2, wild-type mice, but not mutant mice, spent greater time in the target location than in the averaged analogous non-target areas (platform location, $F_{1,24} = 17.7, P < 0.001$). The dashed line represents chance level, corresponding to the ratio of the target area to the total pool area (2.6%). * $P < 0.05$ compared to wild-type mice, within the same platform location; ### $P < 0.01$, #### $P < 0.001$ compared to the target location, within the same genotype. Data are presented as mean \pm SEM.

Figure S6. Behavioral responses in mutant mice treated with D-serine (600 mg/kg) or clozapine (0.75 mg/kg). **(A)** Exploratory activity during sociability session of the social affiliations task. Mean number of chamber entries were similar in wild-type (+/+) and mutant mice (Y269*/Y269*) treated with vehicle (n = 10, 10), D-serine (n = 8, 9), or clozapine (n = 10, 11), indicating comparable chamber exploration. **(B)** In a test of olfactory acuity, the mean latency to dig a buried food pellet did not differ in wild-type and mutant mice given vehicle (n = 11, 10), D-serine (n = 10, 8), or clozapine (n = 10, 7), demonstrating that the drug treatments did not affect olfactory ability. **(C)** Mean startle amplitude in response to a stimulus (120 dB) given without a preceding prepulse. Startle responses in wild-type and mutant mice were not affected by administration of vehicle (n = 9, 11), D-serine (n = 9, 12), or clozapine (n = 9, 8). **(D)** Mean number of beam breaks during the empty open field session (S1) of the object recognition task for wild-type and mutant mice treated with vehicle (n = 9, 10), D-serine (n = 9, 8), and clozapine (n = 10, 9). # $P < 0.05$ compared to vehicle-treated mutant mice. **(E)** Mean duration of locomotor activity in habituation phase (S2-S4), and spatial change session (S5) of the object recognition task did not differ among wild-type and mutant mice injected with vehicle, D-serine, or clozapine. **(F)** In the habituation sessions (S2-S4) of object recognition task, the mean time spent exploring all four objects gradually decreased across sessions in each group (session, $F_{2,98} = 229.4$, $P < 0.001$). No preferential exploration of any individual object was displayed (genotype \times drug treatment \times session \times object, $F_{12,288} = 0.7$, $P = 0.8$). **(G)** In the last habituation session (S4) of the object recognition task, the mean time spent exploring the objects that will be displaced or non-displaced in the subsequent spatial change session did not demonstrate an inherent preference for an object category in any group. **(H)** Mean path length completed to attain a visible (day 1) or hidden platform (acquisition trials, days 2-8) in the MWM. Similar

performance was displayed by wild-type and mutant mice given vehicle ($n = 12, 9$) or D-serine ($n = 11, 8$) during these training trials. Swim speed (genotype \times drug treatment in acquisition trials, $F_{1,37} = 0.6, P = 0.4$), floating ($F_{1,37} = 0.6, P = 0.5$), and thigmotaxis ($F_{1,37} = 0.01, P = 0.9$) did not differ between any group, indicating the presence of normal swimming and motivation. A probe trial was administered 24 h after day 6 and 8, as indicated by an arrow. Mean % time spent in a platform area was examined during probe trials **(I and J)** of the MWM. **(I)** In probe trial 1, vehicle-treated mutant mice displayed a spatial memory deficit that was normalized by D-serine. Mutant mice treated with D-serine spent greater time in the target area than in the averaged analogous non-target locations, similar to wild-type mice given vehicle or D-serine (drug treatment \times platform location, $F_{1,36} = 4.1, P \leq 0.05$). **(II)** In probe trial 2, wild-type mice given vehicle or D-serine and mutant animals given D-serine spent more time over the target platform area than in the averaged analogous non-target locations, whereas vehicle-treated mutant mice did not (drug treatment, $F_{1,36} = 5.8, P < 0.05$; platform location, $F_{1,36} = 13.3, P < 0.001$). The dashed line marks chance level. $*P < 0.05$, $**P < 0.01$ compared to vehicle-treated mutant mice, within the same platform location; $\#P < 0.05$ compared to the target location, within the same genotype and drug treatment group. Data are shown as mean \pm SEM.

Figure S7. Acoustic startle response of mice treated with MK-801 (0.1 mg/kg). Mean startle reactivity (\pm SEM) in response to an acoustic stimulus (120 dB) in the absence of a prepulse. The startle response of mutant animals (Y269*/Y269*) treated with MK-801 ($n = 17$) was elevated in comparison to wild-type mice (+/+) treated with vehicle ($n = 17$) or MK-801 ($n = 16$), and mutant mice given vehicle ($n = 24$) (drug treatment, $F_{1,70} = 7.8, P < 0.01$). $###P < 0.01$ compared to vehicle-treated mutant mice.

Figure S8. Protein levels of genes identified in the microarray analysis. **(A1)** Western blots examining expression of Ttr, Enpp2, Kl, Igf2, Folr1, Prlr, Otx2, and Cldn2 protein in the hippocampus of wild-type (+/+) and mutant (Y269*/Y269*) mice. Significant increases in Ttr, Enpp2, Kl, Igf2, and Prlr protein were found. A trend towards an increased level of Cldn2 protein was also identified ($P = 0.06$). β -Tubulin III was used as a loading control. **(A2)** Densitometric quantification of Western blots for Ttr, Enpp2, Kl, Igf2, Folr1, Prlr, Otx2, and Cldn2. The mean densitometry (\pm SEM) indicates the quantity of measured proteins in wild-type and mutant animals (genotype, $F_{1,4} = 56.3$, $P < 0.01$). * $P < 0.05$, ** $P < 0.01$ compared to wild-type mice, within the same gene.

Figure S9. Linkage disequilibrium plots of four polymorphisms in human *Srr* gene. Nuclear family sample **(A)** and case-control sample **(B)**. In the squares are the D' values, indicating the degree of linkage disequilibrium.

Figure S1

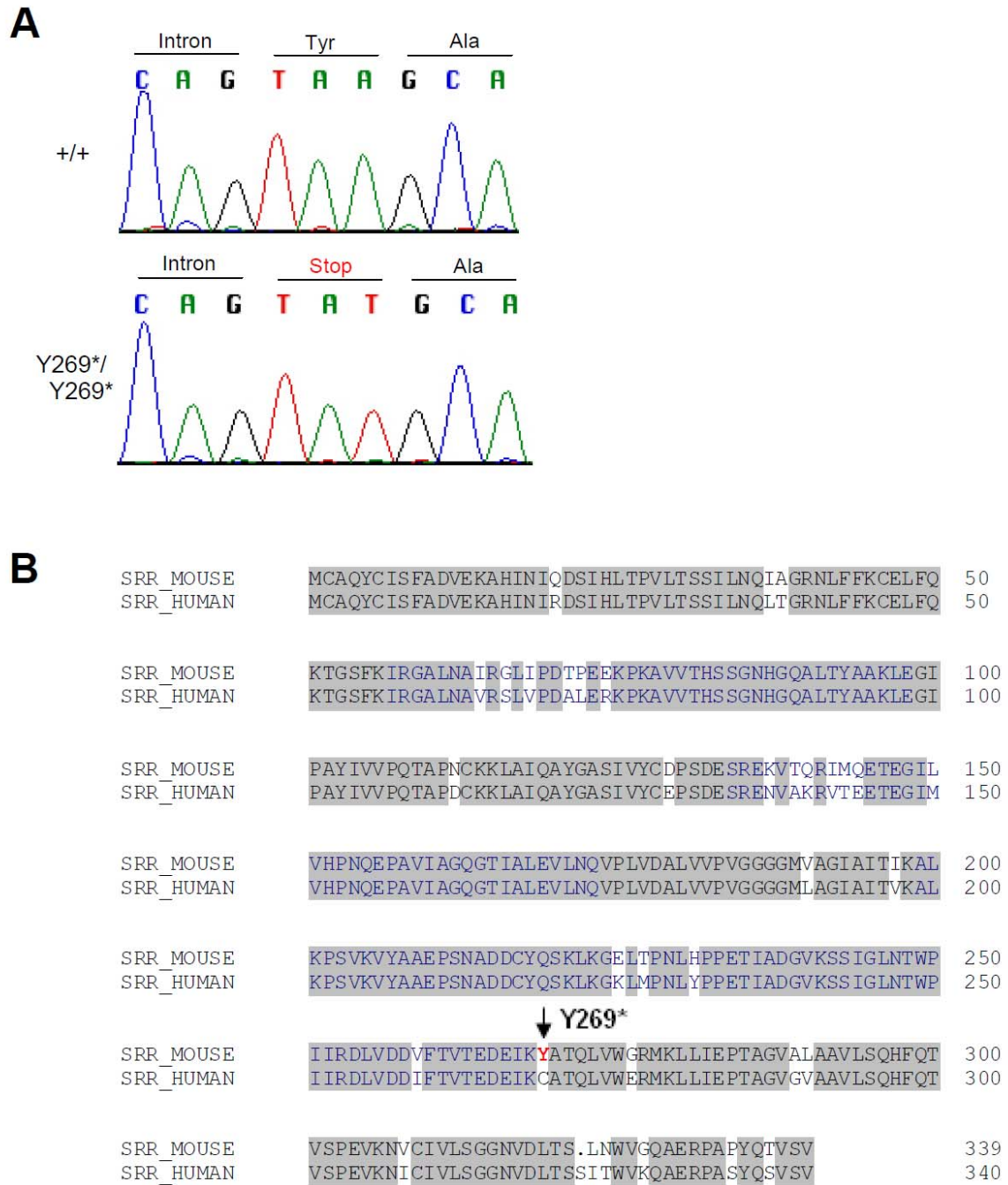
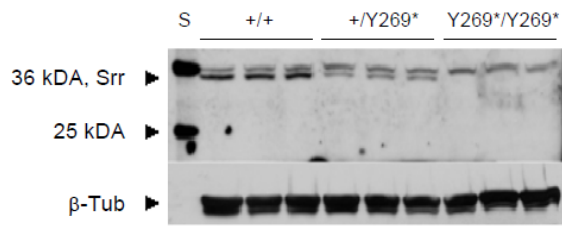
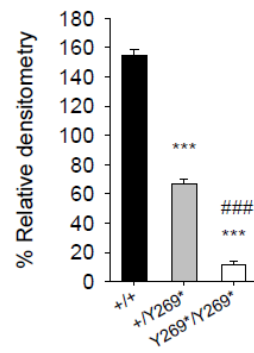


Figure S2

A1



A2



B

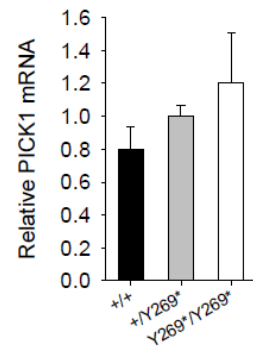


Figure S3

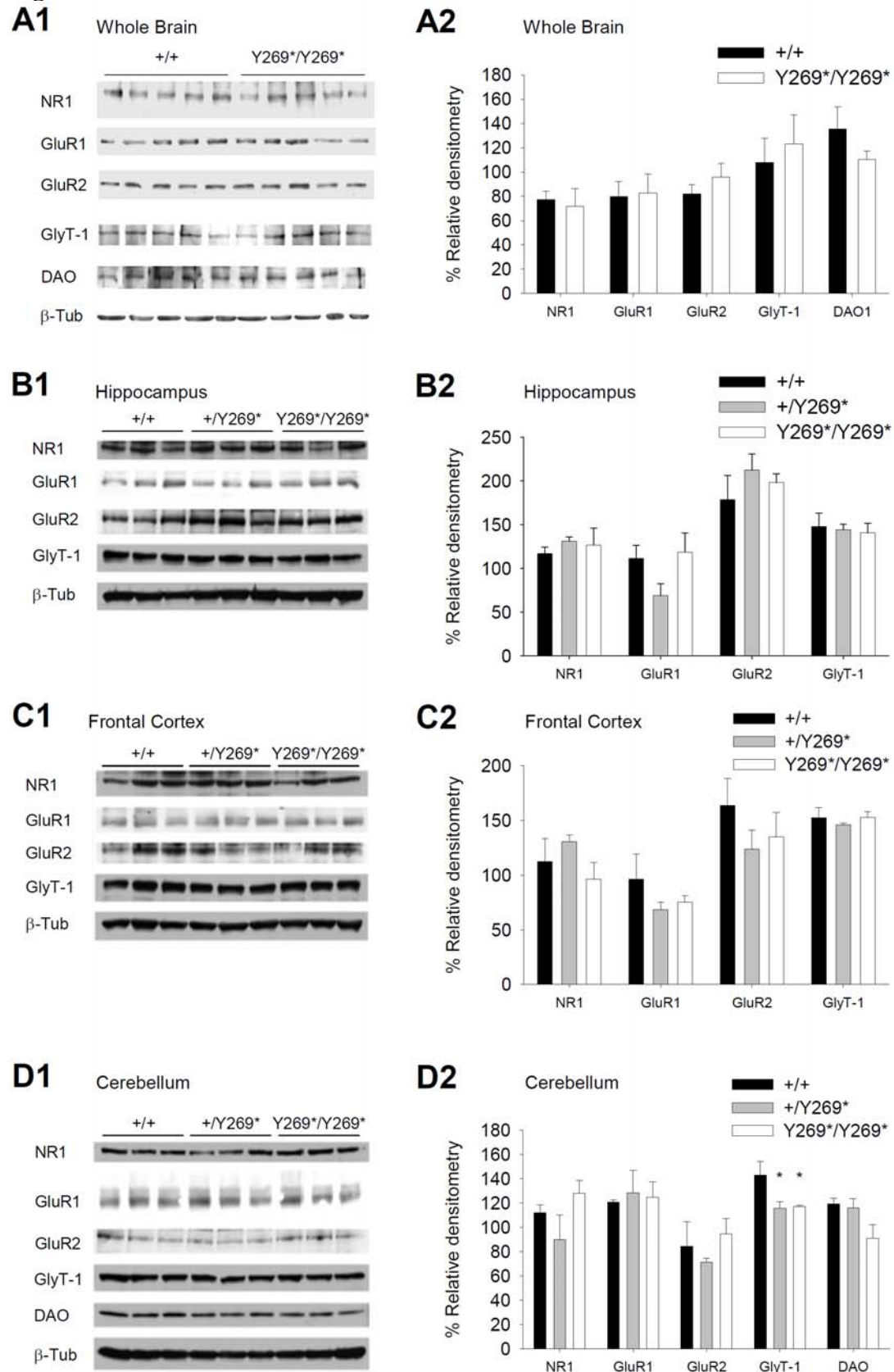


Table S1. HPLC analysis of amino acid concentrations in brain tissue of *Srr^{Y269}* mice

Amino Acid	Whole brain		Frontal cortex		Hippocampus		Cerebellum	
	+/-	Y269*/Y269*	+/-	Y269*/Y269*	+/-	Y269*/Y269*	+/-	Y269*/Y269*
L-serine	60.6 ± 2.8	60.1 ± 1.9	62.2 ± 4.6	84.3 ± 4.6***	69.7 ± 2.6	73.1 ± 1.5	48.5 ± 2.6	50.8 ± 1.8
Glutamate	1776.8 ± 53.6	1699.0 ± 26.1	2119.6 ± 155.1	2455.9 ± 109.6	1632.2 ± 62.1	1605.1 ± 38.5	1510.1 ± 52.7	1591.5 ± 28.1
Glutamine	880.2 ± 32.6	857.4 ± 7.8	894.4 ± 60.8	971.7 ± 48.2	848.4 ± 27.9	769.4 ± 27.6	961.7 ± 30.5	989.4 ± 31.1
Glycine	93.5 ± 3.4	94.8 ± 2.9	57.1 ± 4.8	68.1 ± 4.8	62.0 ± 3.1	60.4 ± 2.6	79.3 ± 5.6	88.1 ± 6.9
Arginine	16.3 ± 1.8	16.2 ± 0.5	8.2 ± 1.0	9.1 ± 0.8	4.6 ± 0.5	3.4 ± 0.4	15.7 ± 0.9	15.5 ± 0.8
Alanine	52.0 ± 4.5	51.9 ± 3.4	59.1 ± 5.4	68.2 ± 4.9	63.7 ± 3.8	62.1 ± 3.5	31.8 ± 1.6	34.8 ± 1.8
GABA	311.7 ± 14.7	291.5 ± 5.7	272.6 ± 18.7	294.8 ± 14.6	296.0 ± 16.3	262.8 ± 12.5	180.0 ± 8.0	190.9 ± 5.6

Data are expressed as mean of amino acid concentration (µg/g tissue ± SEM). n = 5-8 per group.
 ****P* < 0.001 compared to wild-type mice, within the same brain region

Figure S4

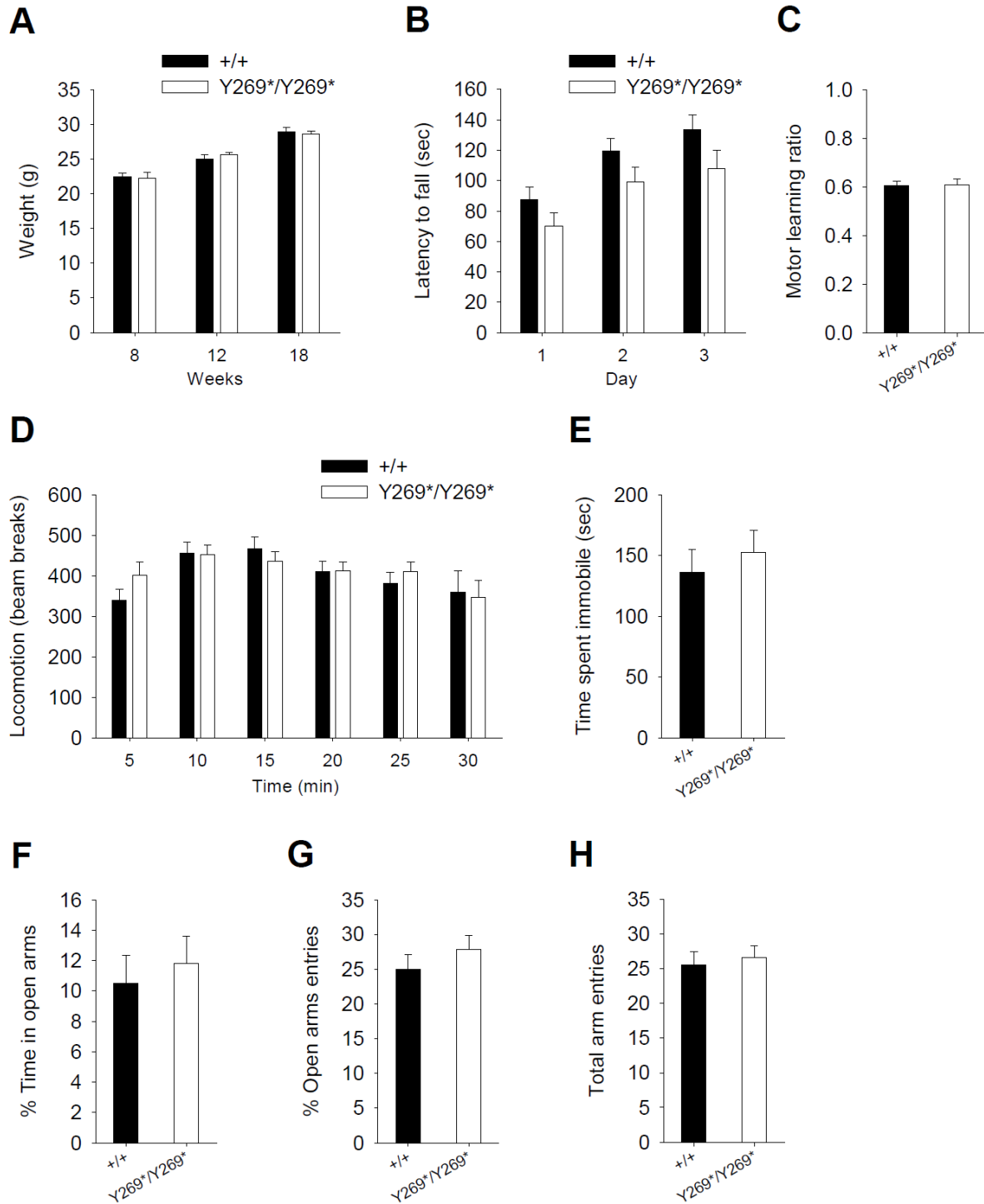


Figure S5

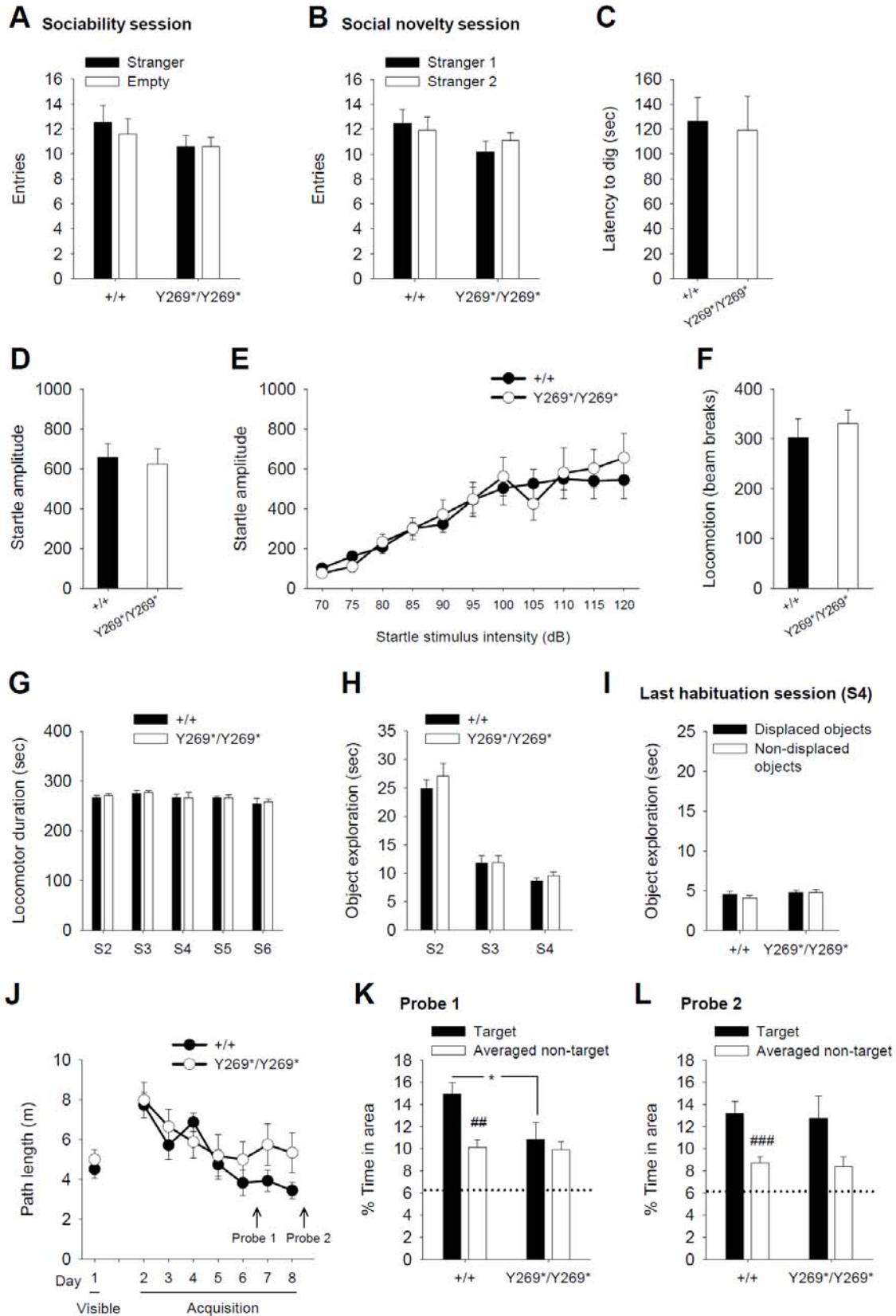


Figure S6

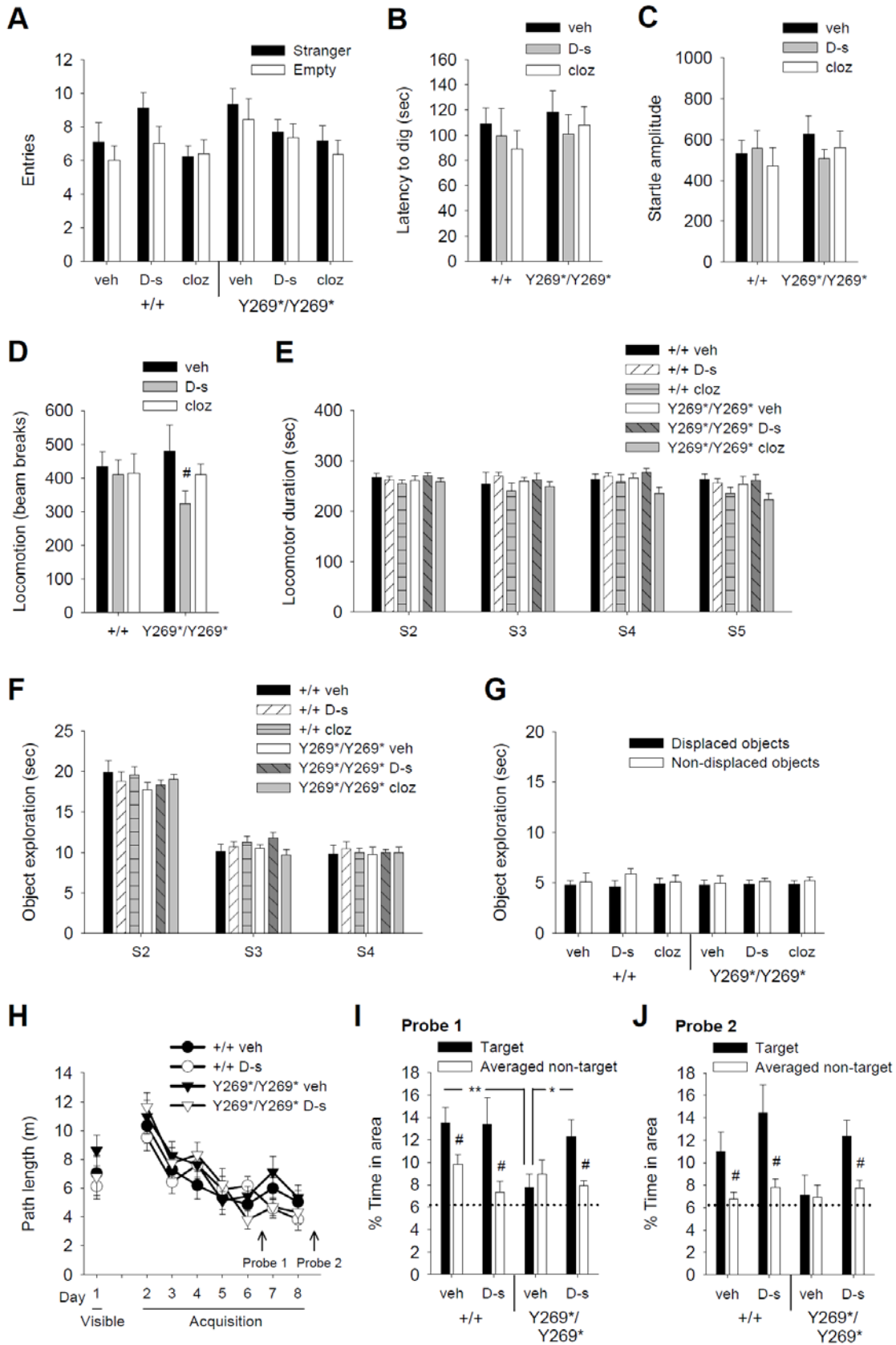


Figure S7

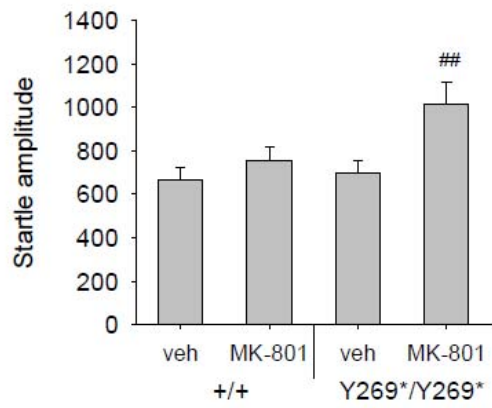


Table S2. Enriched gene ontology categories in *Srr*^{Y269*} mutant mice

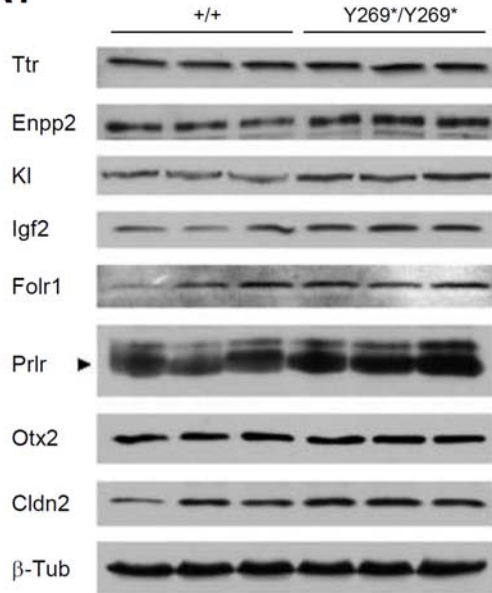
GO ID	GO Category	Fold change		
		Hippocampus	Cerebellum	Frontal Cortex
GO:0005198	Structural molecule activity	3.82*	NS	NS
GO:0005215	Transporter activity	2.58*	NS	NS
GO:0051234	Establishment of localization	2.02*	NS	NS
GO:0044421	Extracellular region part	2.12*	NS	NS
GO:0006810	Transport	2.08*	NS	NS
GO:0051183	Vitamin transporter activity	30.86*	NS	NS
GO:0005615	Extracellular space	2.24*	NS	NS
GO:0005576	Extracellular region	1.88*	NS	NS
GO:0048666	Neuron development	NS	13.81*	NS
GO:0031175	Neurite development	NS	15.74*	NS
GO:0030030	Cell projection organization and biogenesis	NS	11.52*	NS
GO:0032990	Cell part morphogenesis	NS	11.52*	NS
GO:0048858	Cell projection morphogenesis	NS	11.52*	NS
GO:0030182	Neuron differentiation	NS	10.60*	NS
GO:0048667	Neuron morphogenesis during differentiation	NS	14.89*	NS
GO:0048812	Neurite morphogenesis	NS	14.89*	NS
GO:0048699	Generation of neurons	NS	9.34*	NS
GO:0000902	Cell morphogenesis	NS	8.46*	NS
GO:0032989	Cellular structure morphogenesis	NS	8.46*	NS
GO:0000904	Cellular morphogenesis during differentiation	NS	13.20*	NS
GO:0022008	Neurogenesis	NS	8.80*	NS
GO:0007399	Nervous system development	NS	6.16*	NS
GO:0015669	Gas transport	NS	NS	86.98*
GO:0048731	System development	NS	NS	3.63*
GO:0005833	Hemoglobin complex	NS	NS	188.46*
GO:0015671	Oxygen transport	NS	NS	94.2 [†]
GO:0005344	Oxygen transporter activity	NS	NS	102.8 [†]
GO:0019825	Oxygen binding	NS	NS	125.6 [†]

* $P < 0.05$, [†] trend $P < 0.06$ compared to wild-type mice, within the same brain region.

The genes whose mRNA levels were altered by the *Srr* mutation were separately subjected to a Gene Ontology (GO) enrichment analysis to identify perturbed functional groups or pathways.

Figure S8

A1



A2

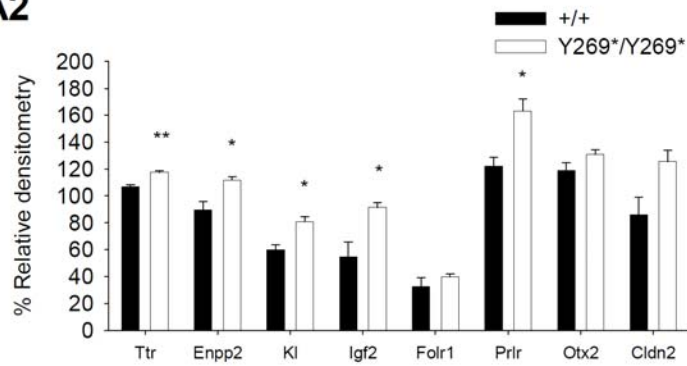
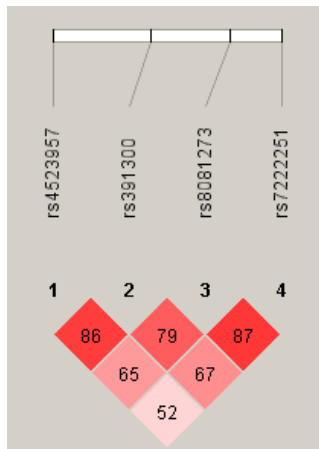


Figure S9

A



B

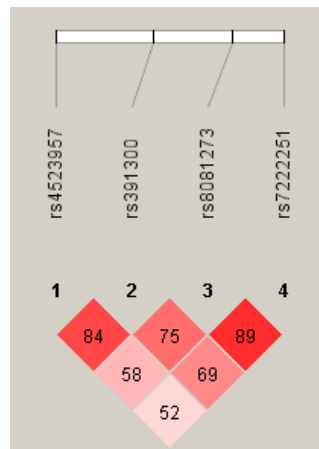


Table S3. Genetic analysis of SNP markers in the *SRR* gene and schizophrenia using a paired case-control sample

SNP	Diagnosis	Genotype			χ^2	P-value	Allele		χ^2	P-value
		11	12	13			1	2		
rs4523957 (1 = T, 2 = G)	SCZ	85	81	28	5.34	0.07	251	137	3.67	0.06
	Control	63	99	32			225	163		
rs391300 (1 = A, 2 = G)	SCZ	27	88	82	2.83	0.24	142	252	1.74	0.19
	Control	29	102	66			160	234		
rs8081273 (1 = T, 2 = C)	SCZ	39	92	72	1.96	0.37	170	236	0.02	0.89
	Control	33	106	64			172	234		
rs7222251 (1 = T, 2 = C)	SCZ	99	84	18	0.74	0.69	282	120	0.74	0.39
	Control	107	79	15			293	109		

Table S4. Haplotype analysis of the schizophrenia case-control sample[†]

Haplotype		SCZ	Control	χ^2	<i>P</i> -value	Global <i>P</i> -value
rs4523957- rs391300	T-G	226	204	2.45	0.12	0.22
	G-A	121	141	2.57	0.11	
rs391300- rs8081273	A-C	126	143	1.70	0.19	0.31
	G-T	150	150	0.00	1.00	
	G-C	102	82	2.99	0.08	
rs8081273- rs7222251	T-T	53	73	3.51	0.06	0.23
	T-C	111	96	1.30	0.25	
	C-T	226	220	0.19	0.66	

[†]Rare haplotypes (frequencies less than 0.05) were omitted from haplotype analysis.